

Mechanical Behavior of the Fingertip In The Range of Frequencies and Displacements Relevant to Touch

Michael Wiertlewski^{a,b}, Vincent Hayward^b

^aCEA LIST, *Sensory and Ambient Interfaces Laboratory, Fontenay-Aux-Roses, France.*

^bUPMC Univ Paris 06, UMR 7222, *Institut des Systèmes Intelligents et de Robotique, Paris, France.*

Abstract

It was previously suggested that the mechanical properties of the fingertip could be characterized by elasticity from DC to about 100 Hz and by viscosity above this frequency. Using a specifically designed high mobility probe, we accurately measured the impedance of the fingertips of seven participants under a variety of conditions relevant to purposeful touch. Direct measurements vindicated previous indirect observations. We also characterized the dependency of the fingertip impedance upon normal load, orientation, and time.

Keywords: Fingertip impedance, finger mechanics, skin mechanics

1. Introduction

There is indirect evidence that a fingertip can be represented by a dominantly elastic load up to a frequency of about 100 Hz, beyond which the load presented by the fingertip, by and large, becomes entirely viscous. This evidence was obtained by Cohen et al. (1999, Fig. 6) using stroboscopic illumination to observe the movements of the glabrous skin when excited by a probe vibrating in the range 0.5 to 240 Hz, and with displacements up to 1 mm. They found that the probe had a tendency to decouple from the skin for increasingly smaller probe displacements past a frequency of 80 Hz, which is indicative of phase shift between force and displacement. Lamoré et al. (1986) stimulated mechanoreceptors through conventional sinusoidal excitation and through the amplitude modulation of a 2 kHz carrier. They found that the skin could be represented by a high-pass mechanical filter with a corner frequency at 80 Hz (Lamoré et al., 1986, Fig. 4). These findings are mutually consistent considering that the skin operates as a transmission medium in the latter experiment, whereas it acts as a load in the former. They are also in accordance with earlier results obtained from vibrating the skin of the arm and the thigh (von Gierker et al., 1952), although the finger differs anatomically from these areas. A probe contact area of 2.17 cm², similar to a finger contact surface area, gives a cross-over frequency of 100 Hz (Moore, 1970, Fig. 2).

We hypothesized that the fingertip can be represented in the tangential direction by an elastic load up to about 100 Hz, by a viscous load above, and with negligible inertial contribution over the entire frequency range relevant to touch. To test this hypothesis, we developed a mechanical probe achieving very high mobility (stiffness ≤ 1.2 N/m, damping ≤ 0.5 N·s/m, accelerance $\leq 10^{-3}$ N·s²/m) which

could approximate a source of force when loaded by a fingertip (Wiertlewski & Hayward, 2012).

We found that the tangential elasticity of the index fingertip of seven participants ranged from $0.6 \cdot 10^3$ to $2.0 \cdot 10^3$ N/m, a result that is inline with previous studies. Moreover, we found that the viscosity of the fingertip load ranged from 0.75 to 2.38 N·s/m and that the inertia of the tissues entrained by a light touch ranged from 110 to 230 mg. Viscous forces indeed far dominate the elastic and inertial forces above 100 Hz. We evaluated the effects of the normal load, orientation, and time course of stimulation. Contact mechanics considerations were used to evaluate the effective complex Young modulus of the fingertip tissues.

2. Previous Approaches To The Direct Determination Of Fingertip Mechanics

Hajian & Howe (1997) found that a finger could be represented by a mass-spring-damper system through impulsive testing delivered by a pneumatic piston acting against a finger that underwent significant rigid-body displacement. Since the excitation had little high-frequency energy, the identification was reliable only in the low frequencies. Kern & Werthschützky (2008) used the ‘impedance head’ approach where force and acceleration are simultaneously measured in the proximity of the interface between the probe and the finger. This approach, however, is known to provide unreliable results in the high frequencies, owing to a possible lack of truly co-located measurements (Brownjohn et al., 1980).

Several other studies were performed in quasi-static conditions (Serina et al., 1997; Pawluk & Howe, 1999b; Jindrich et al., 2003). With specific reference to loading through lateral traction, Nakazawa et al. (2000) found the

values of 0.5 N/mm and 2 N·s/m, for elasticity and viscosity respectively. Pataky et al. (2005), using similar methods, modeled the elastic behavior of the fingertip and the relaxation effect and found values of 1 N/mm and 11 s, for stiffness and relaxation duration, respectively.

The computational modeling of the fingertip (Srinivasan, 1989; Serina et al., 1998; Dandekar et al., 2003; Tada & Pai, 2008; Wu et al., 2007) could predict the bulk response from material properties (Silver et al., 2001; Wang & Hayward, 2007; Pan et al., 1997; Gennisson et al., 2004). The results of these studies are dispersed because of the numerous assumptions required to construct and solve the models, not mentioning the lack of anatomical realism that they must contend with (Hauck et al., 2003).

3. Materials and Methods

It is crucial to use an excitation probe that stores little energy compared to that dissipated by the sample. Thus, a probe should have a high mobility compared to that of the sample. The converse approach, to maximize the impedance of the probe so that all the energy is reflected in the sample—the impedance head approach—has the shortcomings alluded to earlier. Other approaches involving air pressure or ultrasonic waves would not do justice to the contact mechanics in effect during tactual behavior.

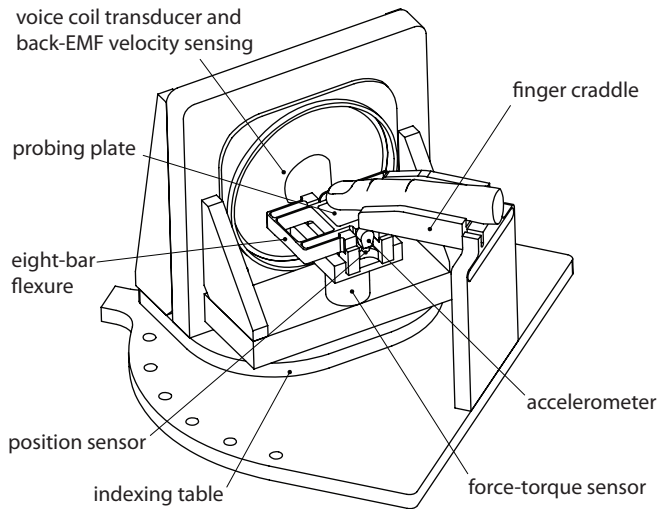


Figure 1: Impedance measurement apparatus.

3.1. Apparatus

The apparatus, see Fig. 1, comprised a probing plate suspended by an eight-bar flexure that guided its movements in the tangential direction. It was stiff in the normal direction. The probe was driven by a voice-coil actuator. To reduce its impedance, position, velocity, and acceleration measurements were fed back, see Fig. 2, where $f_d(t)$ was the interaction force and $\dot{x}(t)$ the velocity. The feedback was tuned to reduced the effective impedance to a small value across the DC-500 Hz range. Let $Y_p = 1/Z_p$

represent the mobility of the probe and Z_c the impedance of the active feedback, the closed-loop impedance of probe was $Z_a = (1 + Y_p Z_p)/Y_p$.

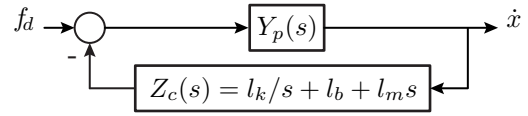


Figure 2: Closed-loop control of the probe implemented with analog electronics feeding back sensed position, velocity and acceleration.

The instrument was supported by a conventional force-torque sensor (Nano 17, ATI Industrial Automation, Apex, NC, USA) to measure the average normal and tangential components of the interaction force. A full description is provided in (Wiertlewski & Hayward, 2012).

The finger was immobilized by a strap onto a hinged cradle permitting the participants to push freely on the probing plate that could be oriented by 15° steps using an indexing table that rotated about a vertical axis. The testing signal, f_d , was a logarithmic frequency sweep and the acceleration, \ddot{x} , was recorded. Using the Fourier transform of the two signals (Welch method), F and \ddot{X} , the impedance Z was computed from,

$$Z(j\omega) = j\omega \frac{F(j\omega)}{\ddot{X}(j\omega)},$$

where $j = \sqrt{-1}$ and ω was the angular pulsation. The impedance of the sample was measured by comparing the unloaded probe response to the loaded response.

3.2. Contact Condition

The contact surface was made from polycarbonate plastic. We first experimented with bonding the fingertip to the plate. This condition created a dependency of the force-displacement curves upon loading or unloading of the contact, owing to a modification of the micromechanics. Estimating that the coefficient friction was higher than 1.2, we restricted the measurement conditions to values where there should be no slip, thereby avoiding the introduction of foreign elements.

3.3. Participants

There were seven volunteer, four males and three females. They gave their informed consent. None of the participant reported any skin condition nor any injury to their fingers. The participants' ages ranged from 23 to 32 with a mean of 25 years.

3.4. Procedure

The participants washed and dried their hands. Their index finger was fastened to the cradle. Before each experimental protocol, the impedance of the unloaded probe was measured 10 times. The mean values and standard deviations were recorded.

Small-Signal Linearity Protocol. Participants regulated the normal force component to 0.5 N via a visual feedback available from a computer screen. Once they could stabilize the desired value, the finger impedance was recorded during a 20–500 Hz frequency sweep lasting 1 s. Proximal-distal and medial-lateral tests were performed. The signal amplitude varied from 0.1 to 0.8 N by steps of 0.1 N.

Normal Force Dependency Protocol. The same frequency sweeps were used but with an amplitude of 0.25 N. Once the participant could remain longer than 10 s within a 10% tolerance range, the data were recorded. The normal force component reference values were 0.25, 0.4, 0.5, 0.6, 0.75, 1.0; 1.25, 1.5, 2.0, 1.5, 1.0, 0.5, and 0.25 N.

Directional Dependency Protocol. The angle between the stimulation direction and the finger proximal-distal axis was varied. The requested normal force component was 0.5 N and measurements were made each 15° in a 180° range. Impedances were recorded from both the left to right and right to left and then averaged to cancel drift in the mechanical properties.

Time Dependency Protocol. To achieve higher temporal resolution, the frequency sweep duration was reduced to 0.25 s and the range to 80–300 Hz. Participants stabilized the pushing force to remain within 10% of 0.5 N. Only medial-lateral stimulation was tested.

Young's Modulus Estimation. To estimate the contact surface area, participants pressed their inked right index finger on a sheet of paper set on a scale. They pressed until reaching a normal force component of 0.5 N. They repeated this procedure four times.

3.5. Data Processing

3.5.1. Lumped Parameters Determination

The fingertip was modeled by a mass-spring-damper system, which gives,

$$Z(j\omega) = b + j \left(m\omega - \frac{k}{\omega} \right),$$

where m is the moving mass, b the viscosity, and k the stiffness. The viscosity was estimated from the real part of the impedance averaged over the whole frequency range. Stiffness and mass were determined using non-linear fitting on the imaginary part of the impedance. A small moving mass cannot be accurately estimated from the above expression. It was more effective to find the frequency at which the imaginary part crosses zero and to estimate the mass from $m = k/\omega^2$.

3.5.2. Effective Young's Modulus

The finger interaction was approximated by a sphere in contact with a flat, rigid surface. Assuming further that the material was linear, isotropic, and homogenous, we

recovered the value of the effective complex modulus from contact mechanics.

For a uniform displacement in the contact area, in polar coordinates, the distribution of traction follows $q(r) = q_0 (1 - r^2/a^2)^{-1/2}$, where a is the contact surface radius and $q_0 = Q/(2\pi a^2)$ is the average traction (Johnson, 1987). The Boussinesq and Cerruti integral of a distributed tangential traction on an elastic half plane with $r < a$ is,

$$\delta = \frac{1}{2\pi G} \iint_S q(\xi, \lambda) \left(\frac{1 - \nu}{\rho} + \nu \frac{(\xi - x)^2}{\rho^3} \right) d\xi d\lambda,$$

where $\rho^2 = (\xi - x)^2 + (\lambda - y)^2$, ν the Poisson coefficient, and G the shear modulus. Young's modulus was found from $G = E/[2(\nu + 1)]$. The evaluation of the above integral with the traction profile, $q_0 (1 - r^2/a^2)^{-1/2}$, leads to an expression for the tangential stiffness, $K = Q/\delta = 8aG/(2 - \nu)$, from which E could be extracted knowing a ($\nu = 0.5$ for soft tissues). To capture the dynamic behavior, we assumed that the stress was a function of the history of deformation (Lee, 1956). For the Kelvin-Voigt model, the stress, $\sigma(t) = E \varepsilon(t) + \eta d\varepsilon(t)/dt$, where ε is the strain and η is the viscosity. When driving the material with an oscillatory motion, the stress and strain were $\sigma(t) = \bar{\sigma} e^{j\omega t}$ and $\varepsilon(t) = \bar{\varepsilon} e^{j\omega t - \phi}$, and the material was represented by a complex modulus $E^* = E + \eta j\omega$. Moduli were extracted from the measurements using $K^*(j\omega) = Z(j\omega) j\omega$ where $K^* = k + b j\omega$ is the complex stiffness.

3.5.3. Contact Surface Area

The fingerprints were imaged using a flat bed scanner. An intensity threshold was used to remove the background and morphological operations filled the holes and cleaned isolated pixels. The resulting binary image was a blob representing the total area of contact. Ellipses were fitted and averaged to recover major and minor axes and hence the equivalent radius of the contact surface.

4. Results

4.1. Frequency Response

An example of the response of the fingertip can be seen in Fig. 3, showing that it could be approximated by a highly damped second-order system with a ≈ 100 Hz corner frequency, justifying the adoption of a Kelvin-Voigt model. The imaginary part exhibited a resonance at 300 Hz indicative of a transition from an elastic regime to an inertial regime, masked in amplitude by damping.

The measurements frequently exhibited high frequency modes (400–500 Hz) in the imaginary part. These modes had a fleeting character. They appeared and vanished seemingly randomly, probably resulting from the establishment and destruction of unstable standing waves in the skin. They were not investigated further.

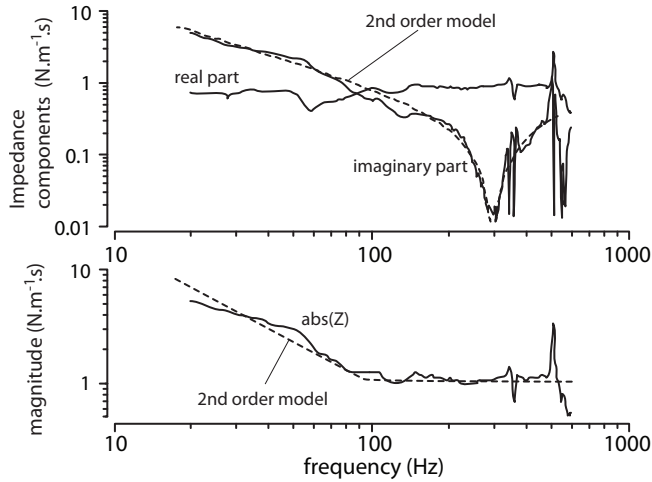


Figure 3: Typical fingertip measurement. The real part represents damping. The imaginary part represents elasticity and inertia. Fitted second-order filter with dominant damping (dashed lines).

4.2. Mechanical Parameters

Table 1 collects the results for all participants. One-way ANOVAs revealed that stiffness, damping, and mass were related to gender ($p=0.026$, $p = 0.001$ and $p=0.0021$ respectively). This dependence was also found for elasticity and viscosity ($p < 0.01$). Stiffness showed a dependency on direction ($p = 0.035$ whereas $p = 0.55$ and $p = 0.37$ for damping and inertia, respectively). Elasticity and viscosity failed to rejected the null hypothesis of correlation with direction ($p = 0.27$ and $p = 0.36$).

Table 1: Dynamic parameters of fingertip, Kelvin-Voigt model for a normal force component magnitude of 0.5 N. The cutoff frequency was calculated from $f = 1/2\pi k/b$.

participant	a mm	k N/mm	b N·s/m	m g	E kPa	η Pa·s	f Hz	R^2
medial-lateral direction								
cr	4.36	0.92	1.52	0.17	118	196	95.8	85
el	4.95	0.94	1.39	0.08	107	158	107.7	89
gt	4.80	1.67	2.38	0.16	195	279	111.2	85
lb	4.82	0.59	1.00	0.11	69	117	93.4	92
ma	4.26	0.75	0.80	0.08	98	106	148.6	93
mw	4.50	0.74	1.26	0.17	92	157	92.9	84
ss	4.40	0.78	0.94	0.12	98	119	130.9	90
proximal-distal direction								
cr	6.27	1.84	1.99	0.23	164	179	146.4	88
el	6.65	1.52	1.53	0.17	127	128	158.3	87
gt	6.14	2.08	2.09	0.23	191	191	158.7	88
lb	7.40	1.10	1.19	0.14	83	90	146.1	83
ma	5.38	0.71	0.75	0.07	74	78	151.3	84
mw	6.20	1.56	1.64	0.18	131	149	151.1	87
ss	6.60	1.23	1.25	0.14	98	106	155.7	90

4.3. Small-Signal Linearity

Position and velocity-force relationships for each participant are shown in Fig. 4. The Spearman correlation

coefficient, ρ , between stiffness and amplitude was always higher than 0.87, except for one outlier, *gt* ($\rho = 0.31$). Damping was also correlated with amplitude as the coefficient was higher than 0.92 for all participants, except for *gt* ($\rho = 0.49$). Linear regressions led to a goodness of fit of $R^2 = 93 \pm 4\%$ for stiffness and $R^2 = 97 \pm 2\%$ for damping.

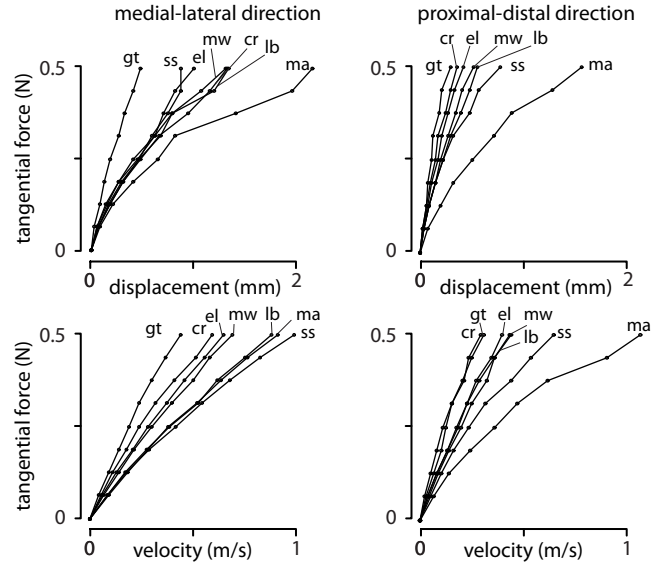


Figure 4: Plots of mechanical parameters values for all participants.

At high amplitudes, it is apparent that stiffness and damping tended to decrease. It is unlikely that this effect was the result of changes in the mechanical properties. It is more probable that partial slip was taking place at high amplitudes.

4.4. Normal Force

The normal force component had impact on all three dynamic parameters, see Fig. 5. Non-parametric Spearman correlation test between force and the parameters gave a minimum value of 0.87 for stiffness and 0.88 for damping. With the exception of three outliers, inertia produced correlations greater than 0.89.

The data were fitted with zero-intercept power-law regressions of the form, βn^α , where α and β are real coefficients and n is the normal force component Table 2. The α coefficients are close to $\frac{1}{3}$, which is consistent with the prediction made by Hertzian contact theory.

Table 2: Power-law coefficients for the stiffness, damping and inertia dependency on normal force. Means \pm s.d.

	α	β	R^2
stiffness [N·mm ⁻¹]	0.35 \pm 0.09	1.48 \pm 0.60	96 \pm 4.5
damping [N·m ⁻¹ ·s]	0.35 \pm 0.10	1.78 \pm 0.60	96 \pm 3.6
mass [g]	0.26 \pm 0.19	0.20 \pm 0.06	71 \pm 20

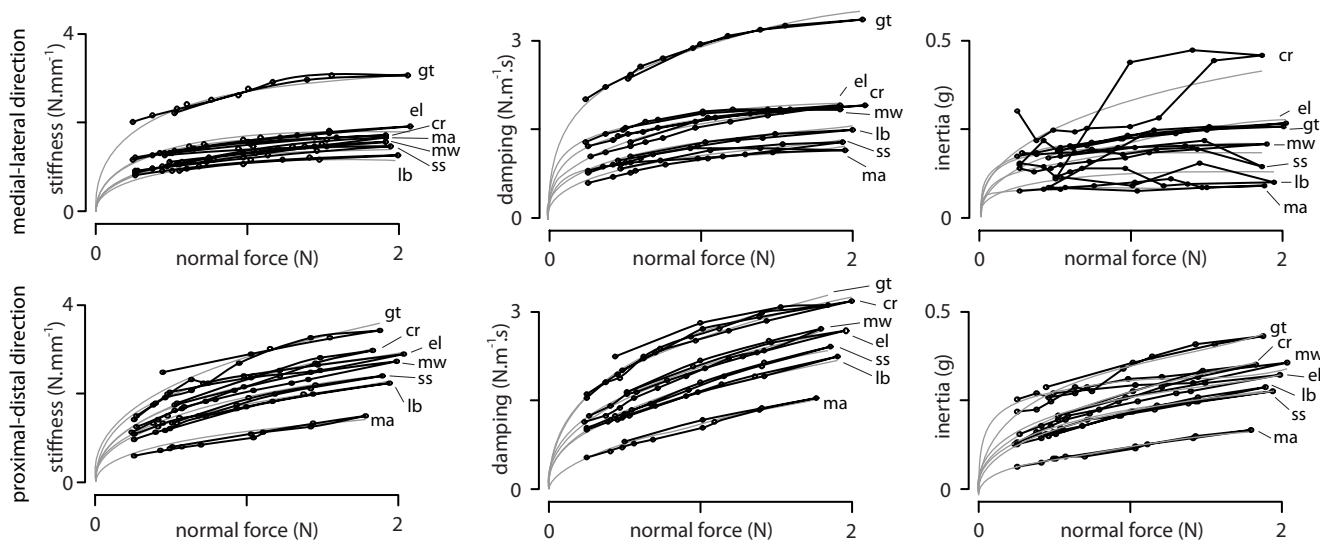


Figure 5: From left to right, stiffness, damping, and inertia, respectively, as a function of normal force for all participants.

4.5. Orientation

Polar plots of the dependency of the mechanical parameters upon orientation for all participants can be inspected in Fig. 6. No two fingers are alike. Participant *ma* has a low-stiffness, low-damping, low-inertia fingertip, unlike *gt*. Participants *lb*, *cr*, *el*, and *ss* exhibited sharp direction tuning of fingertip stiffness. Other had uniform elasticity. A one-way ANOVA showed that stiffness significantly depended on orientation ($p = 0.054$) but the null hypothesis of dependency of damping and inertia on orientation was rejected ($p = 0.95$ and $p = 0.99$ respectively).

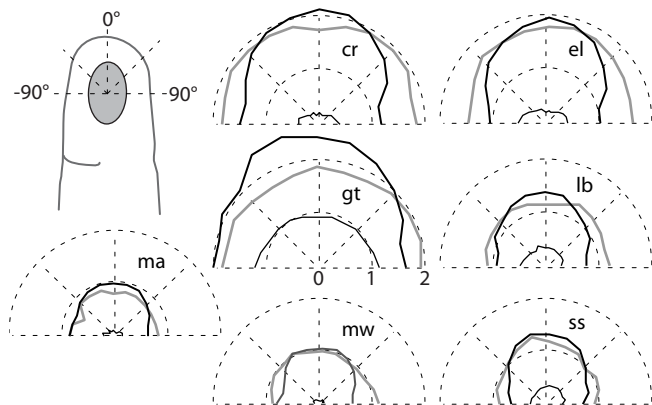


Figure 6: Stiffness [$\text{N}\cdot\text{mm}^{-1}$] (black lines), damping [$\text{N}\cdot\text{m}^{-1}\cdot\text{s}$] (grey lines), and inertia [g] (thinner black lines) as a function of testing direction angle for all participants.

4.6. Time

The high frequencies were not tested in order to enhance the temporal resolution of the measurements. Representative results for a normal force of 0.5 N and 20 s duration of two participants can be seen in Fig. 7.

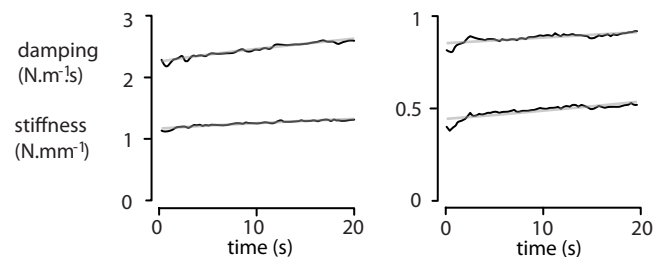


Figure 7: Representative examples for participants *gt* and *lb* of the temporal evolution of stiffness and damping. The gray lines show linear regressions.

For all subjects, Fig. 8 shows the drifts of the mechanical parameters through time. The hypothesis of a correlation of the dynamics properties with time failed to be rejected ($10^{-10} < p < 0.055$).

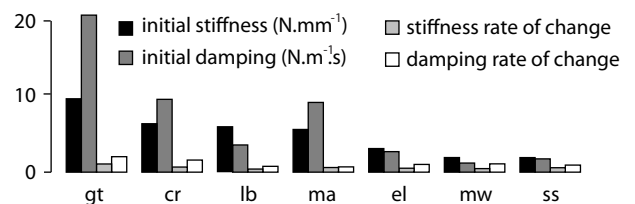


Figure 8: Temporal change of stiffness and damping for all subjects.

5. Discussion

An instrument featuring very high mobility (stiffness lower 1.5 N/m, damping lower than 0.5 N·s/m, and inertia smaller than 1 g) allowed us to measure with high reliability the mechanical impedance of the index fingertip under a variety of loading conditions. Fingertips behaved elastically up to a frequency of about 100 Hz and damping

dominated the interaction beyond this frequency. Inertial contributions could be neglected from DC to 500 Hz.

For some participants, the medial-lateral stiffness could be half of the proximal-distal stiffness but in other participants they were similar. In all participants, however, damping and inertia failed to exhibit marked orientation selectivity. Under normal loading conditions, the lateral stiffness was about 0.8 N/mm and the damping was about 1.2 N·s/m, but these figures can vary greatly among people. When loaded, the mechanical parameters drift upward at a rate of about 0.5% per second. The corner frequency of $(1/2\pi)(800/1.2) \simeq 100$ Hz vindicates the observations of Cohen et al. (1999) and Lamoré et al. (1986).

Assuming uniform bulk mechanics of the fingertip, the effective Young's modulus and viscosity were extracted from contact mechanics considerations. The mean values, 114.9 kPa in medial-lateral direction and 137.5 kPa in the proximal-distal direction, were much lower than previously reported for the skin alone. Wang & Hayward (2007) found a average value of 2.5 MPa for the fingertip skin. Pan et al. (1997) found an average Young's modulus of 458 kPa in the forearm skin. Gennisson et al. (2004) found an average of 2.5 MPa for the skin whereas the epidermis has an elasticity of 10 kPa.

These differences are easy to explain from the fact that the fingertip is a multi-phase structure comprising a fibrous network and multiple anisotropic layers which preclude simple extrapolation of bulk properties from the properties of individual components. In the small-signal, the fingertip behaves essentially like a viscous load at the high frequencies that are characteristic of purposeful touch (Wiertlewski et al., 2011a). Finite element studies suggested that the fingertip resonated at 100–125 Hz (Wu et al., 2007). We did not find any evidence of this phenomenon. Viscous forces swamped out inertial forces over the entire frequency range.

The bulk values that we found are inline with those reported earlier. Nakazawa et al. (2000) found an average damping coefficient in lateral displacement of 2.0 N·s/m (force-step testing) to be compared with the 1.6 N·s/m average found in our study. Viscosity extracted from the contact mechanics considerations is also of the same order than those found with other techniques. The large amount of dissipation can be attributed to fluid displacement in the skin and in subcutaneous tissues (Jamison et al., 1968).

When pushing onto a flat surface, the fingertip area of contact grows rapidly (Serina et al., 1998; Pawluk & Howe, 1999a). The dependence of stiffness, damping, and inertia on the contact surface area mostly followed a $\frac{1}{3}$ power-law, which can be related to Hertz's contact theory. From the small mass that was entrained, viz. 100 mg, we surmise that a very small amount of tissue stores and releases kinetic energy during light contact, and that only must the superficial layers of the fingertip oscillate macroscopically (a 1 mm thick layer over a 1 cm² gives 100 mg). The remaining corresponds to waves dissipating in the body.

Our results bear upon the interpretation of findings re-

lated to the perception of tactual textures which are felt when sliding the fingertips over irregular surfaces. It is accepted that the central nervous system relies on temporal information, i.e. transitory and persisting vibrations generated in the fingertips, at the detriment of spatial information, i.e. strain distributions in the fingertip (Klatzky & Lederman, 1999; Hollins & Bensmaia, 2007).

Viewing the fingertip like a simple solid is a great oversimplification of the actual physics. Studies have shown that the sliding interaction of a fingertip with flat, smoothly undulating, and textured surfaces engendered oscillations having energy in the whole frequency range (Wiertlewski et al., 2011b,a). Large bulk viscosity would be more consistent with the behavior of a bi-phasic solid, suggesting that a fingertip behaves like a filter that attenuates the high spatial frequencies at high temporal frequencies.

Acknowledgment

This work was supported by the French research agency through the REACTIVE project (ANR-07-TECSAN-020). Additional funding was provided by the European Research Council, Advanced Grant PATCH, agreement No. 247300.

- Brownjohn, J. M. W., Steele, G. H., Cawley, P., & Adams, R. D. (1980). Errors in mechanical impedance data obtained with impedance heads. *Journal of Sound and Vibration*, *73*, 461–468.
- Cohen, J. C., Makous, J. C., & Bolanowski, S. J. (1999). Under which conditions do the skin and probe decouple during sinusoidal vibrations? *Experimental Brain Research*, *129*, 211–217.
- Dandekar, K., Raju, B., & Srinivasan, M. (2003). 3-d finite-element models of human and monkey fingertips to investigate the mechanics of tactile sense. *Journal of Biomechanical Engineering*, *125*, 682–691.
- Gennisson, J., Baldeweck, T., Tanter, M., Catheline, S., Fink, M., Sandrin, L., Cornillon, C., & Querleux, B. (2004). Assessment of elastic parameters of human skin using dynamic elastography. *IEEE Transactions on Ultrasonics, Ferroelectrics and Frequency Control*, *51*, 980–989.
- von Gierker, H. E., Oestreicher, H. K., Francke, E. K., Parrack, H. O., & von Wittern, W. W. (1952). Physics of vibrations in living tissues. *Journal of Applied Physiology*, *4*, 886–900.
- Hajian, A., & Howe, R. (1997). Identification of the mechanical impedance at the human finger tip. *Journal of Biomechanical Engineering*, *119*, 109–114.
- Hauck, R. M., Camp, L., Ehrlich, H. P., C., C. G., Sagers, B. S., Banducci, D. R., & Graham, P. W. P. (2003). Pulp nonfiction: Microscopic anatomy of the digital pulp space. *Plastic Reconstructive Surgery*, *113*.
- Hollins, M., & Bensmaia, S. J. (2007). The coding of roughness. *Canadian Journal of Experimental Psychology/Revue canadienne de psychologie experimentale*, *61*, 184–195.
- Jamison, C. E., Marangoni, R. D., & Glaser, A. A. (1968). Viscoelastic properties of soft tissue by discrete model characterization. *Journal of Biomechanics*, *1*, 33–36.
- Jindrich, D., Zhou, Y., Becker, T., & Dennerlein, J. (2003). Non-linear viscoelastic models predict fingertip pulp force-displacement characteristics during voluntary tapping. *Journal of Biomechanics*, *36*, 497–503.
- Johnson, K. (1987). *Contact mechanics*. Cambridge University Press.
- Kern, T. A., & Werthschützky, R. (2008). Studies of the mechanical impedance of the index finger in multiple dimensions. In M. F. et al. (Ed.), *Proceedings of EuroHaptics 2008* (pp. 175–180).

- Klatzky, R., & Lederman, S. (1999). Tactile roughness perception with a rigid link interposed between skin and surface. *Attention, Perception, & Psychophysics*, *61*, 591–607.
- Lamoré, P. J. J., Muijser, H., & Keemink, C. J. (1986). Envelope detection of amplitude-modulated high-frequency sinusoidal signals by skin mechanoreceptors. *Journal of the Acoustical Society of America*, *79*, 1082–1085.
- Lee, E. H. (1956). Stress analysis in viscoelastic materials. *Journal of Applied Physics*, *27*, 665–672.
- Moore, T. J. (1970). A survey of the mechanical characteristics of skin and tissue in response to vibratory stimulation. *IEEE Transactions on Man-Machine Systems*, *11*, 79–84.
- Nakazawa, N., Ikeura, R., & Inooka, H. (2000). Characteristics of human fingertips in the shearing direction. *Biological Cybernetics*, *82*, 207–214.
- Pan, L., Zan, L., & Foster, F. (1997). In vivo high frequency ultrasound assessment of skin elasticity. In *Proceedings of the IEEE Ultrasonics Symposium* (pp. 1087–1091). volume 2.
- Pataky, T. C., Latash, M. L., & Zatsiorsky, V. M. (2005). Viscoelastic response of the finger pad to incremental tangential displacements. *Journal of Biomechanics*, *38*, 1441–1449.
- Pawluk, D. T. V., & Howe, R. D. (1999a). Dynamic contact of the human fingerpad against a flat surface. *Journal of Biomechanical Engineering*, *121*, 605–611.
- Pawluk, D. T. V., & Howe, R. D. (1999b). Dynamic lumped element response of the human fingerpad. *Transactions of the ASME*, *121*, 178–183.
- Serina, E., Mockensturm, E., Mote Jr, C. D., & Rempel, D. (1998). A structural model of the forced compression of the fingertip pulp. *Journal of Biomechanics*, *31*, 639–646.
- Serina, E. R., Mote, C. D., & Rempel, D. (1997). Force response of the fingertip pulp to repeated compression—effects of loading rate, loading angle and anthropometry. *Journal of Biomechanics*, *30*, 1035–1040.
- Silver, F. H., Freeman, J. W., & DeVore, D. (2001). Viscoelastic properties of human skin and processed dermis. *Skin Research and Technology*, *7*, 18–23.
- Srinivasan, M. A. (1989). Surface deflection of primate fingertip under line load. *Journal of Biomechanics*, *22*, 343–349.
- Tada, M., & Pai, D. (2008). Finger shell: Predicting finger pad deformation under line loading. In *Proceedings of the Symposium on Haptic Interfaces for Virtual Environments and Teleoperator Systems* (pp. 107–112).
- Wang, Q., & Hayward, V. (2007). In vivo biomechanics of the fingerpad skin under local tangential traction. *Journal of Biomechanics*, *40*, 851–860.
- Wiertelwski, M., & Hayward, V. (2012). Transducer for mechanical impedance testing over a wide frequency range through active feedback. *Review of Scientific Instruments*, in press.
- Wiertelwski, M., Hudin, C., & Hayward, V. (2011a). On the 1/f noise and non-integer harmonic decay of the interaction of a finger sliding on flat and sinusoidal surfaces. In *Proceedings of World Haptics Conference 2011* (pp. 25–30).
- Wiertelwski, M., Lozada, J., & Hayward, V. (2011b). The spatial spectrum of tangential skin displacement can encode tactual texture. *IEEE Transactions on Robotics*, *27*, 461–472.
- Wu, J. Z., Welcome, D. E., Krajnak, K., & Dong, R. G. (2007). Finite element analysis of the penetrations of shear and normal vibrations into the soft tissues in a fingertip. *Medical Engineering & Physics*, *29*, 718–727.